JOURNAL OF PROPULSION AND POWER
Vol. 9, No. 2, March–April 1993

Reduced-Length Scarfed-Nozzles for Thrust Vector Adjustment

Jay S. Lilley*
U.S. Army Missile Command, Redstone Arsenal, Alabama 35898

The results of an investigation into the utilization of scarfed, truncated perfect-nozzles for thrust vector adjustment in tactical strap-on boosters is presented. The use of truncated perfect-nozzle expansion contours was evaluated as a means of achieving significant nozzle length reductions over conical nozzle designs without degrading axial thrust or thrust vector adjustment capability. Previously developed perfect-nozzle and scarfed-nozzle performance analysis computer codes were used to generate an extensive parametric study which characterized the influence of nozzle length and expansion ratio on axial thrust and thrust vector adjustment capability. Comparisons were made against the results obtained for scarfed-nozzles with conical expansion contours. The parametric study was utilized to develop a general scarfed truncated perfect-nozzle design methodology. This methodology was exercised to generate a specific reduced-length scarfed-nozzle design. The axial performance and thrust vector adjustment capability of the nozzle design was experimentally verified through solid rocket motor static firings.

Nomenclature

A = downstream throat attachment point
A_t = throat area
C_F = thrust coefficient
E = scarfed extension starting point
F = scarfed extension ending point
G = perfect-nozzle exit plane
M = side force action point
P = pressure
R = ratio
T = throat point
t = time
X = motor axial coordinate
x = nozzle axial coordinate
Y = motor radial coordinate
y = nozzle radial coordinate
α = wall angle, basic nozzle half-angle
β = scarf angle
γ = specific heat ratio
ε = expansion ratio
η = discrepancy
θ_T = thrust angle
ρ = throat curvature radius

Subscripts

a = ambient
ave = time averaged
e = scarfed extension starting point
exp = averaged and corrected to reference conditions
F = thrust
f = scarfed extension ending point
g = perfect-nozzle exit plane
L = length
m = side force action point
per = perfect-nozzle
ref = reference
req = required
t = stagnation, throat
td = throat downstream
theo = theoretical
tu = throat upstream
X = motor axial coordinate
x = nozzle axial coordinate
Y = motor radial coordinate
y = nozzle radial coordinate
θ = thrust angle

Received July 30, 1990; revision received Oct. 16, 1992; accepted for publication Oct. 19, 1992.

*Aerospace Engineer, Propulsion Directorate. Senior Member AIAA.

Introduction

FOR certain tactical missile designs it is desirable to employ several strap-on solid rocket boosters attached circumferentially around a centerbody. This propulsion system concept creates significant problems for the missile designer as the performance of each individual booster will be subject to the motor-to-motor variability in thrust level and burn time that is characteristic of solid rocket motors. This variability will generate significant moments which will have an adverse impact on the design of the guidance and control system for the missile.

The obvious method to eliminate the moments generated by the propulsion system is to adjust the thrust vector for each individual booster so that it passes through the missile center of gravity. An attractive thrust vector adjustment approach is to employ scarfed-nozzles on each booster. These scarfed-nozzles consist of a conventional axisymmetric nozzle which has a truncated (scarfed) cylindrical extension attached downstream. An extensive investigation into the application of scarfed-nozzles for thrust vector adjustment was conducted by Lilley and Arszman.[1] In this investigation, the thrust vector adjustment capability of scarfed-nozzles employing conical expansion contours was theoretically and experimentally demonstrated. A conceptual illustration of the booster concept is presented in Ref. 1.

Most tactical missile systems have severe constraints on the volume allocated to the propulsion system, and it is desirable to reduce nozzle length. A means of achieving this length reduction is to utilize a nonconical nozzle expansion contour which offers significant length reductions without the flow divergence performance degradation that results from increasing the half-angle of a conical nozzle. Extensive investigations have been conducted to determine nozzle expansion contours which minimize the axial length that is required to produce a given thrust level. Through calculus of variation techniques, Rao[2] determined unique optimum nozzle contours that offered the minimum length for a given thrust level and expansion ratio. Ahlberg et al.[3] conducted an alternative investigation into utilizing truncated perfect-nozzles to achieve reduced expansion contour lengths. While the contours de-

termined by Rao represented the mathematical optimum solution, Ahlberg demonstrated that truncated perfect-nozzles yielded performance levels that were essentially equivalent to those produced by the optimum contours. Consequently, significant nozzle length reduction could be achieved utilizing either Rao or truncated perfect-nozzle contours.

An attractive feature of truncated perfect-nozzles is the relative simplicity of the contour generation process. For a fixed throat geometry and specific heat ratio, the only independent design parameter for a perfect-nozzle is the expansion ratio at which parallel uniform flow is achieved. In contrast, to specify a Rao nozzle (with fixed throat geometry and specific heat ratio) two design parameters are required (i.e., thrust and expansion ratio). This simplicity of perfect-nozzle construction allows the designer to generate a universal family of nozzle contours for a wide range of expansion ratios that can be utilized to generate an extensive matrix of truncated perfect-nozzle designs. To evaluate a corresponding matrix employing Rao nozzles, a significantly greater number of nozzle contours must be generated. To achieve greater flexibility and simplicity in performing nozzle design studies (at the expense of not utilizing the mathematically optimum contours), truncated perfect-nozzles were selected as the nonconical nozzle design approach to be investigated.

An investigation was conducted to evaluate the performance of scarfed truncated perfect-nozzles for thrust vector adjustment. Previous investigations demonstrated the thrust vector adjustment capability of scarfed-nozzles.[1] However, these studies utilized conical scarfed-nozzles and did not address the issue of length reduction. Another previous investigation presented the length reduction advantages of utilizing scarfed perfect-nozzles.[4] However, that study considered side-existing canted nozzles and did not address thrust vector adjustment. The current study consequently utilized the previous work as a point of departure by incorporation of all relevant results, design methodologies, and analysis tools. Previously developed theoretical performance analysis models [4,5] were utilized to generate perfect-nozzle contours and to predict scarfed-nozzle performance. Utilizing these models, a parametric study was conducted to investigate the influence of nozzle length and expansion ratio on axial thrust and thrust vector adjustment capability. The results of the parametric study were compared against those obtained in the previous investigation for conical expansion contours[1] to demonstrate the length reduction advantages of using truncated perfect-nozzle contours. The parametric study was employed as the basis of a general methodology for generating scarfed truncated perfect-nozzle designs. This methodology was illustrated through a specific nozzle design example. This design example was then experimentally validated through static firings of specially configured solid rocket motors.

Theoretical Investigation

In order to determine the relative merits of employing truncated perfect-nozzle expansion contours on scarfed-nozzles utilized for thrust vector adjustment, a theoretical parametric study was conducted to characterize the performance of such nozzles.

Performance Model

The scarfed-nozzle geometric model employed in the present investigation is illustrated in Fig. 1. The scarfed-nozzle is composed of three distinct sections: 1) the throat, 2) the basic nozzle, and 3) the nozzle extension. The nozzle geometric model is described in detail in Ref. 5. The analysis tools utilized in this investigation are two nozzle performance prediction computer codes developed by Hoffman.[5] The first tool is a perfect-nozzle design/analysis code which was exercised extensively in the investigation presented in Ref. 4, and a complete description of theoretical basis for the code is presented in Ref. 6. The second tool is a scarfed-nozzle analysis code which has served as the principal scarfed-nozzle analysis

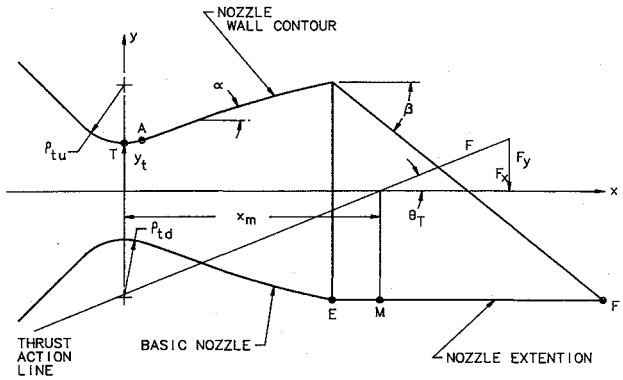

Fig. 1 Scarfed-nozzle geometric model.

tool for a number of previous investigations[1,7-10] and is described in detail in Ref. 5.

The performance factors which are of principal importance are the motor axial thrust coefficient, $C_{F,X}$, and the thrust angle, θ_T, which are given by the following relationships:

$$C_{F,X} = F_X/(P_t A_t) \tag{1}$$

$$\theta_T = \tan^{-1}(F_Y/F_X) \tag{2}$$

Where F_X is the motor axial thrust, F_Y is the motor side thrust, P_t is the stagnation pressure, and A_t is the nozzle throat area.

Parametric Study

To characterize the performance of truncated perfect-nozzles with scarfed cylindrical extensions, an extensive parametric design study was performed. For each scarfed-nozzle evaluated in this study, the throat profile was specified by $\rho_{tu}/y_t = 1.0$ and $\rho_{td}/y_t = 0.5$ and the specific heat ratio was $\gamma = 1.2$. These values were selected as typical for tactical solid rocket motors, and they are the same as those utilized in the previous investigation presented in Ref. 1. To standardize the performance predictions, vacuum operating conditions were selected ($P_a/P_t = 0$ where P_a is the ambient pressure). Employing this set of inputs, the perfect-nozzle design/analysis code was utilized to generate 160 perfect-nozzle contours and their associated wall pressure distributions. The contours were generated for ε_{per} from 1.5 to 60. The perfect-nozzle expansion ratio is defined by the following relationship:

$$\varepsilon_{per} = (y_g/y_t)^2 \tag{3}$$

where point G is the nozzle axial station where parallel uniform flow is achieved.

For the parametric study, the following independent variables were identified; basic nozzle ε, β, basic nozzle contour (conical or truncated perfect), and basic nozzle length x_e/y_t. The following set of expansion ratios was selected for evaluation:

$$\varepsilon = 2.0, 2.5, 3.0, 3.5, 4.0, 4.5, 5.0, 5.5, 6.0, 6.5, 7.0, 7.5, 8.0, 8.5, 9.0, 9.5, 10.0$$

where

$$\varepsilon = (y_e/y_t)^2 \tag{4}$$

For the parametric study, a β of 30 deg was selected to provide the longest practical length for scarfed extensions, and represented a maximum thrust vector adjustment capability.

Each of the 160 perfect-nozzle contours was truncated at every specified ε value that did not exceed the original ε_{per} value, and corresponding axial performance calculations were made. The sets of truncated perfect-nozzles that corresponded to each ε value were then utilized to obtain specific scarfed-nozzle geometries for analysis. For each ε value, truncated perfect-nozzle contours were identified and generated that had equivalent basic nozzle lengths (x_e/y_t) to conical nozzles with half-angles of 10, 15, 20, and 25 deg. In addition, for each ε value, truncated perfect-nozzle contours were identified and generated that had equivalent axial performance ($C_{F,X}$) to the same four conical basic nozzles. Thus, for each ε value, the design/analysis code was utilized to generate eight new perfect-nozzle designs which were truncated to the appropriate expansion ratios. These eight designs were then used as input to the scarfed-nozzle performance prediction code and scarfed-nozzle performance predictions were generated for each.

Results

The objective of the present investigation was to evaluate the advantages of utilizing truncated perfect basic nozzle contours on scarfed-nozzles utilized for thrust vector adjustment. To clearly demonstrate these advantages, the results of the current investigation were compared against the baseline performance result determined for conical nozzles in the previous investigation. The results of the present parametric study are presented in terms of R_L, R_F, and R_θ which are given by the following relationships:

$$R_L = (x_e/y_t)/(x_e/y_t)_{\text{ref}} \tag{5}$$

$$R_F = C_{F,X}/C_{F,X_{\text{ref}}} \tag{6}$$

$$R_\theta = \theta_T/\theta_{T_{\text{ref}}} \tag{7}$$

where the subscript ref denotes the values for the baseline reference nozzle. For each ε value, the corresponding conical basic nozzle with a 10-deg half-angle was selected as the reference scarfed-nozzle design. Presented in Table 1 are the specifications for the reference nozzles. Presented in Figs. 2–4 are typical results from the parametric study. Presented in Fig. 2 is a plot of thrust ratio as a function of length ratio for selected expansion ratios. Results are presented for both conical (labeled "con") and perfect (labeled "per") basic nozzles. The conical performance points are for half-angles of 10, 15, 20, 25, and 30 deg. Presented in Fig. 3 is a plot of thrust angle ratio as a function of length ratio for the same expansion ratios. Once again, both conical and truncated perfect basic nozzle results are presented. The conical points are for half-angles of 10, 15, 20, and 25 deg. Presented in Fig. 4 is a plot of perfect-nozzle expansion ratio as a function of length ratio for the same expansion ratios.

From the results presented in Figs. 2–4, the following general observations can be made about scarfed-nozzles with a fixed expansion ratio:

1) For a fixed thrust level (R_F value) the basic nozzle with the truncated perfect-nozzle contour will be shorter than conical basic nozzle.

2) For a fixed basic nozzle length (R_L value) the basic nozzle with the truncated perfect-nozzle contour will have higher performance than the conical basic nozzle.

3) As basic nozzle length decreases, the thrust level of the truncated perfect-nozzle approaches that of the conical nozzle.

4) The performance advantage (or conversely length reduction advantage) of the truncated perfect-nozzle becomes more significant as expansion ratio is increased.

5) For a fixed basic nozzle length, the conical nozzle has a greater thrust vector adjustment capability.

Table 1 Reference vacuum performance values for 10-deg conical nozzles

ε	$C_{F,X_{\text{ref}}}$	$X_{e_{\text{ref}}}/y_t$	$\theta_{T_{\text{ref}}}$, deg
2.0	1.4469	2.3929	15.8783
2.5	1.4951	3.3395	14.2915
3.0	1.5286	4.1954	13.2911
3.5	1.5545	4.9825	12.4913
4.0	1.5779	5.7150	11.6821
4.5	1.5994	6.4031	11.0303
5.0	1.6173	7.0538	10.5334
5.5	1.6327	7.6728	10.1197
6.0	1.6462	8.2642	9.7734
6.5	1.6580	8.8315	9.4722
7.0	1.6685	9.3773	9.2380
7.5	1.6779	9.9039	9.0459
8.0	1.6865	10.4133	8.8587
8.5	1.6943	10.9069	8.7299
9.0	1.7015	11.3863	8.5804
9.5	1.7082	11.8525	8.4056
10.0	1.7413	12.3066	8.3157

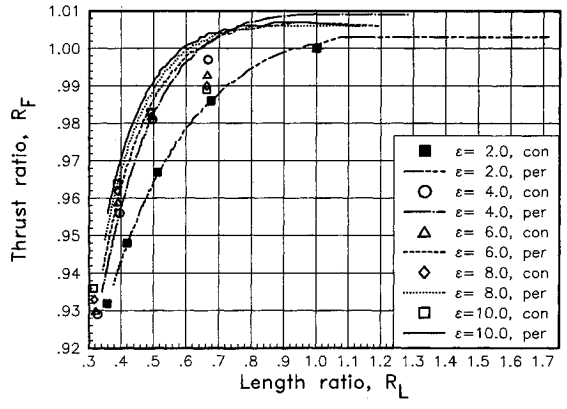

Fig. 2 R_F as a function of R_L for P_a = 0.0.

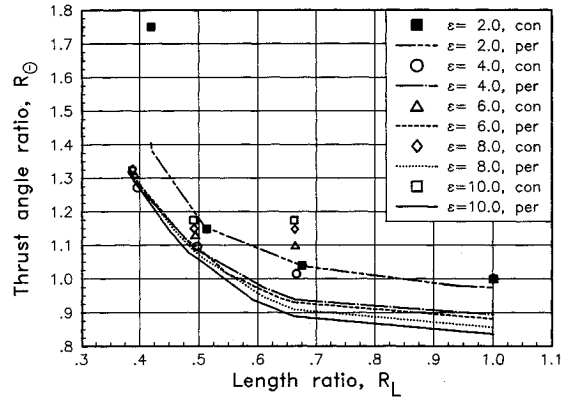

Fig. 3 R_θ as a function of R_L for P_a = 0.0.

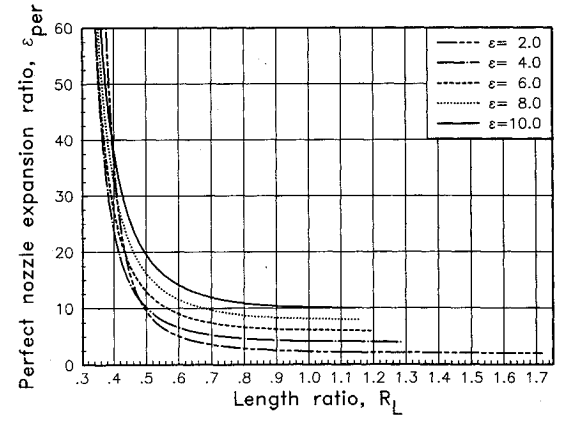

Fig. 4 ε_{per} as a function of R_L.

6) As basic nozzle length decreases, the thrust vector adjustment capability of the truncated perfect-nozzle approaches that of the conical nozzle.

7) The thrust vector adjustment advantage of the conical nozzle becomes more significant as expansion ratio is increased.

It is apparent that the use of a truncated perfect-nozzle contour results in a thrust level increase over an equivalent length conical nozzle ($R_L = 1.0$). Conversely, the use of a truncated perfect-nozzle provides a length reduction over an equivalent thrust conical nozzle ($R_F = 1.0$). In both cases there is a reduction in thrust vector adjustment capability. The two obvious questions that must be answered by the nozzle designer are: is it more desirable to have higher axial performance in the same length or reduced length and the same axial performance; and is the thrust vector adjustment capability of the selected truncated perfect scarfed-nozzle design sufficient?

If the case of equivalent length nozzles is considered, it can be seen from the results in Figs. 2–4 that the performance gains achieved with truncated perfect-nozzle are minimal. Over the range of expansion ratios considered, a truncated nozzle that is equivalent in length to a 10 deg conical nozzle will provide a thrust improvement of less than 1%. If the case of equivalent thrust nozzles is considered, it is evident that significant nozzle length reductions are available. For the range of expansion ratios considered, a truncated perfect-nozzle that had equivalent thrust to a 10 deg conical nozzle would provide a nozzle length reduction of 6–61%. For tactical missile systems where the length of the nozzle is likely to be a significant portion of the overall rocket motor length, the equivalent thrust design approach is the superior alternative.

With regard to thrust vector adjustment capability, the results in Figs. 2–4 show that over the range of expansion ratios considered, truncated perfect nozzles that have equivalent thrust to 10 deg conical nozzles will have a degradation of thrust vector adjustment of 2–6%. This degradation is small and the thrust vector capability for all the 10 deg equivalent thrust nozzles exceeds 8.7 deg. This capability is more than adequate for most tactical booster applications.

Nozzle Design Methodology

The results of the parametric study provide a general format for the design of a scarfed perfect-nozzle for thrust vector adjustment applications. The assumption is made that a preliminary booster design utilizing a conical (reference) scarfed-nozzle has been produced and an improved reduced length nozzle design is desired. The following are assumed to be known:

Motor operating conditions—P_t, P_a, γ

Nozzle geometry constraints—y_t, ρ_{tu}/y_t, ρ_{td}/y_t, ε

Reference performance—$C_{F,X_{ref}}$, $\theta_{T_{ref}}$

Reference geometry—$\theta_{T_{ref}}$

Required thrust vector angle—$\theta_{T_{req}}$

Utilizing the motor operating conditions and the nozzle geometry requirements, the perfect-nozzle design/analysis code is employed to generate a series of perfect-nozzle designs and the associated performance predictions. Utilizing these designs, the performance and geometry of the reference nozzle, and Eqs. (5) and (6), a plot of R_F as a function of R_L is generated. The results of this plot are interpolated to determine ε_{per} at which equivalent thrust ($R_F = 1.0$) is achieved. Once ε_{per} value has been determined, the corresponding perfect-nozzle contour is generated. The perfect-nozzle contour is truncated and used as input to the scarfed-nozzle performance prediction code to determine the thrust vector adjustment capability. The result is a reduced-length nozzle design.

Nozzle Design Example

To illustrate the use of the design methodology, the previously detailed procedure was exercised to produce an improved scarfed-nozzle design.

The reference motor operating conditions are as follows: $P_t = 3400$ psia, $P_a = 14.7$ psia, $\gamma = 1.2$. The nozzle geometry constraints are $y_t = 0.415$ in., $\rho_{tu} = 10.0$ in., $\rho_{td} = 0.010$ in., $y_e = 0.415$ in., $\varepsilon = 4.8612$. The reference nozzle has a 12-deg half-angle, and the related performance and geometric values are presented in Table 2. The required thrust vector adjustment angle is $\theta_{T_{req}} = 5.4$ deg.

Utilizing the motor operating conditions and nozzle geometry constraints, perfect nozzle contours were generated for 77 perfect-nozzle expansion ratios ($\varepsilon_{per} = 4.8612$, 5.0–20.0 in increments of 0.2). Presented in Fig. 5 is the plot of R_F as a function of R_L that was generated from the perfect-nozzle contours analysis results. Also presented in Fig. 5 are design points for conical nozzles with half-angles of 12, 15, 20, 25, and 30 deg. Presented in Fig. 6 is a plot of ε_{per} as a function of R_L. Using the results in Figs. 5 and 6, the equivalent thrust nozzle design was determined, generated, and evaluated. A performance and geometrical comparison between the reference and improved design is presented in Table

Table 2 Nozzle design comparison

	Baseline, 12-deg cone	Improved, perfect
$C_{F,X}$	1.5981	1.6002
x_e/y_t	5.6695	3.9237
θ_T, deg	10.473	9.386
R_L	1.000	0.6921
R_θ	1.0000	0.8962
R_F	1.000	1.000
ε_{per}	——	7.5708

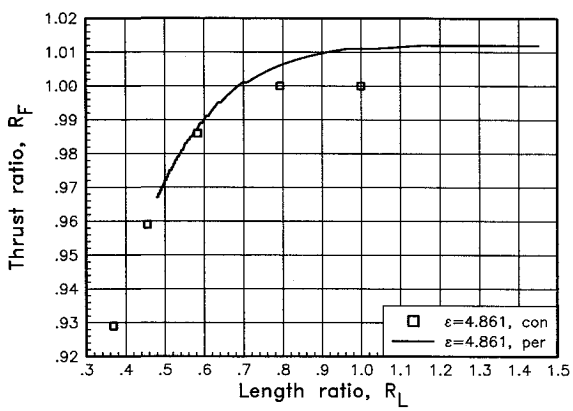

Fig. 5 R_F as a function of R_L for design example ($\varepsilon = 4.861$, $P_a/P_t = 0.0043$).

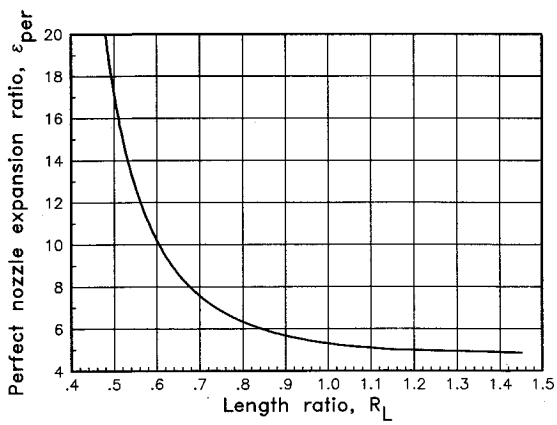

Fig. 6 ε_{per} as a function of R_L for design example.

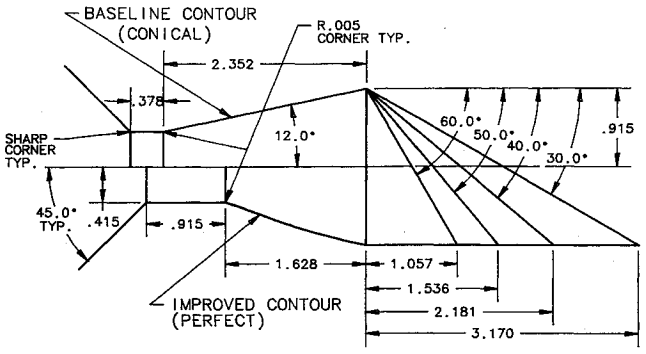

Fig. 7 Design example baseline and improved nozzle configurations.

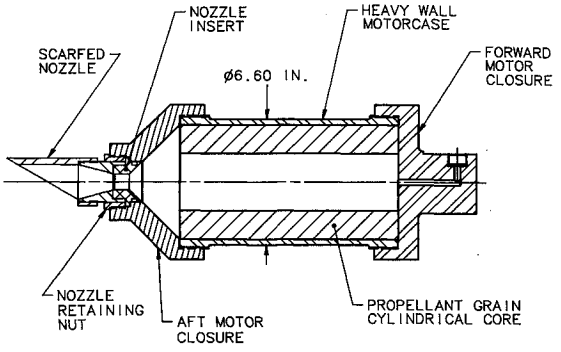

Fig. 8 Solid rocket motor cross section.

2. Presented in Fig. 7 are cross-sectional drawings of both nozzle designs.

From the results presented in Table 2, it is evident that the perfect-nozzle design offers significant length reduction over the conical baseline. By utilizing the improved design, a 30.8% basic nozzle length reduction can be achieved while maintaining an equivalent thrust level. In addition, the improved design has a thrust vector angle of 9.4 deg which exceeds the 5.4-deg requirement.

Experimental Evaluation

An experimental evaluation effort was conducted to validate the analysis tools and the design methodology through verification of the design example.

Setup/Hardware

The nozzle geometries generated in the design example were experimentally evaluated through solid rocket motor firings. Existing heavy-wall, solid rocket motor hardware was configured with a single, removable, scarfed-nozzle that was oriented coaxial to the motor axis. The propellant formulation and cylindrical port grain configuration were designed to provide a nominal chamber pressure of 3400 psia when the nozzle geometries illustrated in Fig. 7 were utilized. Presented in Fig. 8 is a cross section of the rocket motor. The motor was mounted vertically on a six-component thrust stand which was an integral unit capable of independently measuring three force and three moment components.

Eight motor firings were conducted. Both the baseline and the improved nozzles from the design example were each evaluated with cylindrical nozzle extensions that had scarf angles of 30, 40, 50, and 60 deg. The primary objectives of these evaluations were to experimentally verify the following 1) the ability to predict axial thrust for both designs; 2) the ability to predict thrust angle for both designs; 3) that the improved design has equivalent motor axial thrust to the baseline design; 4) that the thrust vector can be adjusted by varying the scarf angle; and 5) that the axial performance of both designs is independent of the scarfed extension geometry.

Cross-sectional drawings of the nominal nozzle geometries that were used are presented in Fig. 7. Presented in Table 3 are the nozzle configurations that correspond to each test. For each motor firing a theoretical scarfed-nozzle performance analysis was conducted for the reference operating conditions.

Data Analysis

In order to consistently analyze the data from the test program, the experimental results from each test were time-averaged and the performance values were adjusted to the reference operating conditions (as presented in the design example). The burn time for each test was defined as the period of time where the motor chamber pressure exceeds 70% of the maximum value achieved. The data averaging period for each test was selected as the first 0.50 s of the motor burn time. This averaging period was selected to minimize the impact of nozzle erosion on the data. The averaged performance data were adjusted to the reference operating conditions. This adjustment process is described in Ref. 1. The averaged and adjusted results for each test are presented in Table 3.

To perform comparisons between theoretical and experimental results, η_F and η_θ are also presented in Table 3. These discrepancies are determined from the following relationships:

$$\eta_F = C_{F,X_{\text{exp}}}/C_{F,X_{\text{theo}}} \tag{8}$$

$$\eta_\theta = \theta_{T_{\text{exp}}}/\theta_{T_{\text{theo}}} \tag{9}$$

To provide additional insight into the thrust vector adjustment capability, shown in Fig. 9 is a plot of thrust angle as a function of scarf angle for the reference pressure levels. Both theoretical (denoted "theo") and corrected experimental (denoted "exp") are presented for both conical and truncated perfect-nozzles. The theoretical and experimental values of β_{req} that satisfies $\theta_{T_{\text{req}}}$ of 5.4 deg for the conical contour, are 56.5 and 49.4 deg, respectively. For the perfect contour, the required scarf angles are 57.1 and 53.3 deg, respectively.

The results in Table 3 and Fig. 9 were utilized to assess the degree to which the objectives of the experimental verification effort were satisfied. The following are those assessments:

1) The results indicate a general agreement between the theoretical predictions for motor axial performance and the experimental values. For all tests the predicted motor axial thrust coefficient was within 12% of the experimental value. In all tests the performance model over-predicted the motor axial thrust coefficient. These apparent performance losses (as compared to theoretical results) can be primarily attributed to unmodeled factors such as heat transfer through the nozzle wall, boundary-layer effects, and two phase flow. The level of agreement achieved is consistent with that demonstrated on the previous studies in which the performance models were utilized to predict the thrust of the small solid rocket motors employing scarfed-nozzles.[1,7,9,10] For the small nozzles (in the size class considered in this study) the impact on thrust of the previously mentioned unmodeled factors typically result in overpredictions on the order of 10%. However, if the designer is cognizant of the bias introduced by these unmodeled factors, the performance models can be adjusted (calibrated) to produce accurate thrust predictions.

2) The results indicate a qualitative agreement between the theoretical predictions for thrust angle and the experimental values. For all tests the predicted thrust angle was within 22% of the experimental value. For both basic nozzle configurations, the performance model over-predicted the thrust angle for small scarf angles (30 deg) and underpredicted the thrust angle for large scarf angles (60 deg). The relatively higher level of disagreement between experimental and theoretical thrust angles (as compared to the axial thrust efficiencies) and the observed inconsistencies can be attributed to the fact that

Table 3 Test results summary

	Averaged data, first 0.50 s of burn				Averaged data corrected to reference conditions		Theoretical performance at reference conditions		Discrepancies	
Test	β, deg	$P_{t_{ave}}$, psia	$C_{F,X}$, ave	$\theta_{T_{ave}}$, deg	$C_{F,X}$, exp	$\theta_{T_{exp}}$, deg	$C_{F,X_{theo}}$	$\theta_{T_{theo}}$, deg	η_F	η_θ
C-1	30	3958	1.4500	11.11	1.4470	10.99	1.5981	10.46	0.91	1.05
C-2	40	4428	1.4524	8.44	1.4475	8.15	1.5981	8.26	0.91	0.99
C-3	50	3580	1.4285	5.27	1.4275	5.21	1.5981	6.33	0.89	0.82
C-4	60	3410	1.4034	3.84	1.4034	3.84	1.5981	4.90	0.88	0.78
P-1	30	2826	1.5457	9.40	1.5500	9.68	1.5981	9.39	0.97	1.03
P-2	40	2841	1.5480	8.17	1.5521	8.42	1.5981	7.68	0.97	1.10
P-3	50	2940	1.4649	5.59	1.4682	5.81	1.5981	6.30	0.92	0.92
P-4	60	2909	1.4534	4.32	1.4570	4.56	1.5981	5.03	0.91	0.91

C Test series—conical contours. P Test series—perfect contours.
ave—Experimental data that has been time averaged over the first 0.50 sec of the burn time for the given test.
exp—Experimental data that has been time averaged and then adjusted to the reference conditions.
theo—Theoretical performance predictions based on the reference conditions.

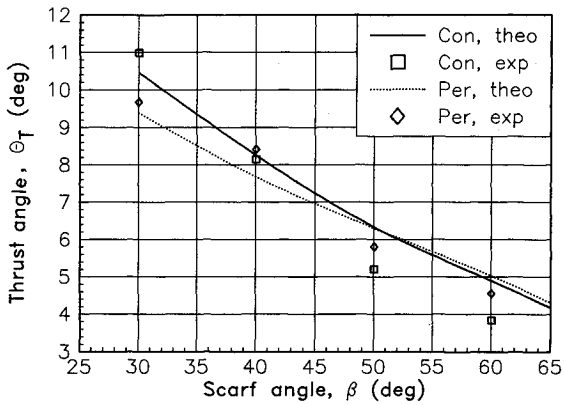

Fig. 9 Thrust angle vs scarf angle.

the thrust angle is based on two independent thrust components [see Eq. (2)]. Consequently, the inaccuracies and inconsistencies in predicting the two independent thrust values both contribute to the final predicted thrust angle. However, the significant observation that can be made from the results in Table 3, is that for both nozzle contours, the theoretical model qualitatively predicted the influence of scarf angle on thrust angle as is clearly illustrated in Fig. 9.

3) The results experimentally verify that the motor axial performance of the improved nozzle is equivalent (or superior) to that of the baseline design. The adjusted average axial thrust coefficient for all four perfect-nozzle tests were superior to those of the four conical nozzle tests.

4) The results experimentally verify that the thrust angle can be adjusted through changes in the scarf angle. These results experimentally verify that, for the baseline design, a continuum of thrust of angles from 0 to 11 deg can be achieved, and that for the improved design, a continuum from 0 to 9.7 deg is available. The results in Fig. 9 verify that both nozzles have a demonstrated range of thrust vector adjustment capability that satisfies the required design thrust angle of 5.4 deg.

5) The results experimentally verify that the motor axial performance of both nozzle designs is independent of the scarfed extension geometry. For the baseline design, the axial performance of tests C-1 and C-2 were equivalent. The axial performance of tests C-3 and C-4 were also equivalent to each other, but at a degraded level as compared to the first two tests. This trend, which holds for the improved nozzles as well, is a direct result of the testing sequence and not the scarfed-nozzle geometry. For the no. 1 and 2 tests, for both nozzle configurations, new nozzle hardware was utilized (throats, expansion contours, and scarfed extensions). For the no. 3 and 4 tests, the previously used throats and expansion contours were refurbished and utilized with new scarfed extensions. Consequently, the performance degradation observed for the second pair of tests for each contour was most likely a result of the nozzle hardware having been fired once. The influence of scarfed extension geometry on motor axial performance is evaluated by comparing, for each nozzle contour, the relative performance of the no. 1 test against that of the no. 2 test and the axial performance of the no. 3 test against that of the no. 4 test. From the results in Table 3 it is clear that the influence is negligible, and that axial performance is independent of scarfed extension geometry.

Conclusions

Existing design and analysis tools were utilized to investigate the performance of scarfed perfect-nozzles for thrust vector adjustment. These models were exercised for a wide range of nozzle lengths and expansion ratios. The results of this theoretical study indicate that for a given expansion ratio, the use of a truncated perfect-nozzle contour will result in a significant reduction in basic nozzle lengths as compared to a 10-deg conical nozzle. This length reduction is achieved with no degradation in axial thrust and a substantial thrust vector adjustment capability. The analysis models and the results of the theoretical study were utilized to develop a scarfed perfect-nozzle design methodology. The application of this methodology was illustrated through a specific design example. The nozzle design generated in the example was utilized in an experimental effort which validated the analysis tools and the design methodology.

For many tactical rocket motor applications, the nozzle design is constrained by overall geometry, cost, and motor design requirements. The results of the previous investigation demonstrated that scarfed-nozzles offer the propulsion system designer a low-cost, high-performance means of thrust vector adjustment. The results of the present investigation demonstrate that use of perfect nozzle contours provides significant length reductions without sacrificing the above benefits.

Acknowledgments

The author wishes to express his appreciation to the personnel of the Propulsion Directorate of the U.S. Army Missile Command, who provided invaluable support on this program in terms of hardware fabrication and assembly, propellant development and casting, and data acquisition and reduction.

References

[1]Lilley, J. S., and Arszman, J. H., "The Application of Scarfed Nozzles for Thrust Vector Adjustment," *Journal of Propulsion and Power*, Vol. 7, No. 3, 1991, pp. 382–388.

[2]Rao, G. V. R., "Exhaust Nozzle Contour for Optimum Thrust," *Jet Propulsion*, Vol. 28, No. 6, 1958, pp. 377–382.

[3]Ahlberg, J. H., Hamilton, D. M., and Nilson, E. M., "Truncated Perfect Nozzles in Optimum Nozzle Design," *Journal of the American Rocket Society*, Vol. 31, No. 5, 1961, pp. 614–620.

[4]Lilley, J. S., "Optimum Geometries for Scarfed Perfect Nozzles," *Journal of Propulsion and Power*, Vol. 7, No. 4, 1991, pp. 586–592.

[5]Hoffman, J. D., "A Computer Program for the Performance Analysis of Scarfed Nozzles," U.S. Army Missile Command, RK-CR-84-3, Redstone Arsenal, AL, May 1984.

[6]Zucrow, M. J., and Hoffman, J. D., *Gas Dynamics*, Vol. II, Wiley, New York, 1977, pp. 160–164.

[7]Lilley J. S., and Hoffman, J., "Performance Analysis of Scarfed Nozzles," *Journal of Spacecraft and Rockets*, Vol. 23, No. 1, 1986, p. 53–62.

[8]Lilley, J. S., "The Design and Optimization of Propulsion Systems Employing Scarfed Nozzles," *Journal of Spacecraft and Rockets*, Vol. 23, No. 6, 1986, pp. 597–604.

[9]Lilley, J. S., "Experimental Validation of a Performance Model for Scarfed Nozzles," *Journal of Spacecraft and Rockets*, Vol. 24, No. 6, 1987, pp. 474–480.

[10]Lilley, J. S., "The Analysis and Design of Scarfed Nozzles for Tactical Applications," U.S. Army Missile Command, TR-RD-PR-86-2, Redstone Arsenal, AL, Oct. 1986.

[11]Lilley, J. S., "Scarfed Perfect Nozzles for Thrust Vector Adjustment in Tactical Strap-On Boosters," AIAA Paper 90-2210, July 1990.